Text and references accompanying Nevada Bureau of Mines and Geology Map 166

Overview of the Stratigraphy and Structure of the Iceberg Canyon Quadrangle, Clark County, Nevada and Mohave County, Arizona

Robert J. Brady[1], Joan E. Fryxell[2], and Brian P. Wernicke[3]

[1]Department of Geology and Geophysics, University of Calgary, Calgary, AB, Canada
[2]Department of Geological Sciences, California State University, San Bernardino
[3]Division of Geological and Planetary Sciences, California Institute of Technology, Pasadena

INTRODUCTION

The Iceberg Canyon quadrangle exposes a crystalline basement complex of deformed Paleoproterozoic gneisses which are intruded by the Mesoproterozoic Gold Butte Granite, and unconformably overlying cover sequences consisting of Paleozoic cratonal sedimentary strata and Neogene nonmarine sedimentary and volcanic rocks. Deformation within the map area can be broken into two major intervals: (1) a Proterozoic interval that is poorly understood and expressed as a complex pattern of meso- and micro-scale folding and faulting of the crystalline basement, and (2) a Neogene interval of west–northwest directed extension that generated a set of dominantly west-dipping normal faults and related folds. This Neogene extension is interpreted to be the earliest Basin and Range extension at this latitude, and the resulting structures dominate the physiography of the region.

The purpose of this report is to provide an overview of the stratigraphy and structural geology of the Iceberg Canyon quadrangle, and discuss the current understanding of the timing of deformation and how the observed deformation fits into the regional pattern. Further discussion of the geology of the Iceberg Canyon quadrangle, as well as surrounding portions of the southern Virgin Mountains and Colorado Plateau can be found in Longwell (1936), Bowyer (1958), Volborth (1962), Lucchitta (1966), Morgan (1968), Matthews (1976), Bohannon (1984), Lucchitta and Young (1986), Fitzgerald et al. (1991), Fryxell et al. (1992), Beard (1996), Brady (1998), Duebendorfer and Sharp (1998), Brady et al. (2000), Reiners et al. (2000), Anderson et al. (2001), Faulds et al. (2001a), Howard et al. (2003), and Wallace et al. (2005).

GEOLOGIC SETTING

The Iceberg Canyon quadrangle includes the southeastern portion of the southern Virgin Mountains, as well as parts of the Grand Wash trough, Gregg Basin, Iceberg Canyon, and Grand Wash Bay portion of Lake Mead, along with various smaller bays and coves (figures 1, 2). Elevations within the quadrangle range from lake level (normally 366 m, but potentially anywhere from original river level of ~265 m to the Boulder Dam spillway elevation of 372.3 m) up to a peak elevation of 1351 m in the northwestern part.

The quadrangle is located in southeastern Nevada and northwestern Arizona, near the eastern margin of the highly extended central Basin and Range province and at the northern end of the Colorado River extensional corridor (figure 1). The Colorado River extensional corridor is bounded on its eastern edge by the relatively undeformed Colorado Plateau, which is only ~5 km east of the map area. The northern boundary of the extensional corridor is formed by the right-lateral Las Vegas Valley shear zone and left-lateral Lake Mead fault zone. The trace of the Gold Butte fault, which is generally considered to be the southeasternmost strand of the Lake Mead fault system, trends in a WSW–ENE direction only ~5 km north of the map area (figure 2). The western boundary of the northern Colorado River extensional corridor is formed by the relatively unextended Spring Mountains, which are located ~115 km west of the quadrangle.

Although the Iceberg Canyon quadrangle does not include the breakaway fault(s) that defines the sharp transition from essentially unextended crust of the Colorado Plateau to highly extended crust of the Basin and Range province, that fault(s) must be directly adjacent to the eastern edge of the quadrangle, buried within the Grand Wash trough. Middle Miocene and older rocks within the quadrangle are affected by large magnitude extension, and the crystalline basement on the western side of the quadrangle is the footwall to the South Virgin–White Hills detachment fault, which is a large-offset normal fault that is interpreted to have accommodated >10 km of west-side-down normal displacement (Fitzgerald et al., 1991; Fryxell et al., 1992; Brady, 1998; Duebendorfer and Sharp, 1998; Brady et al., 2000; Reiners et al., 2000).

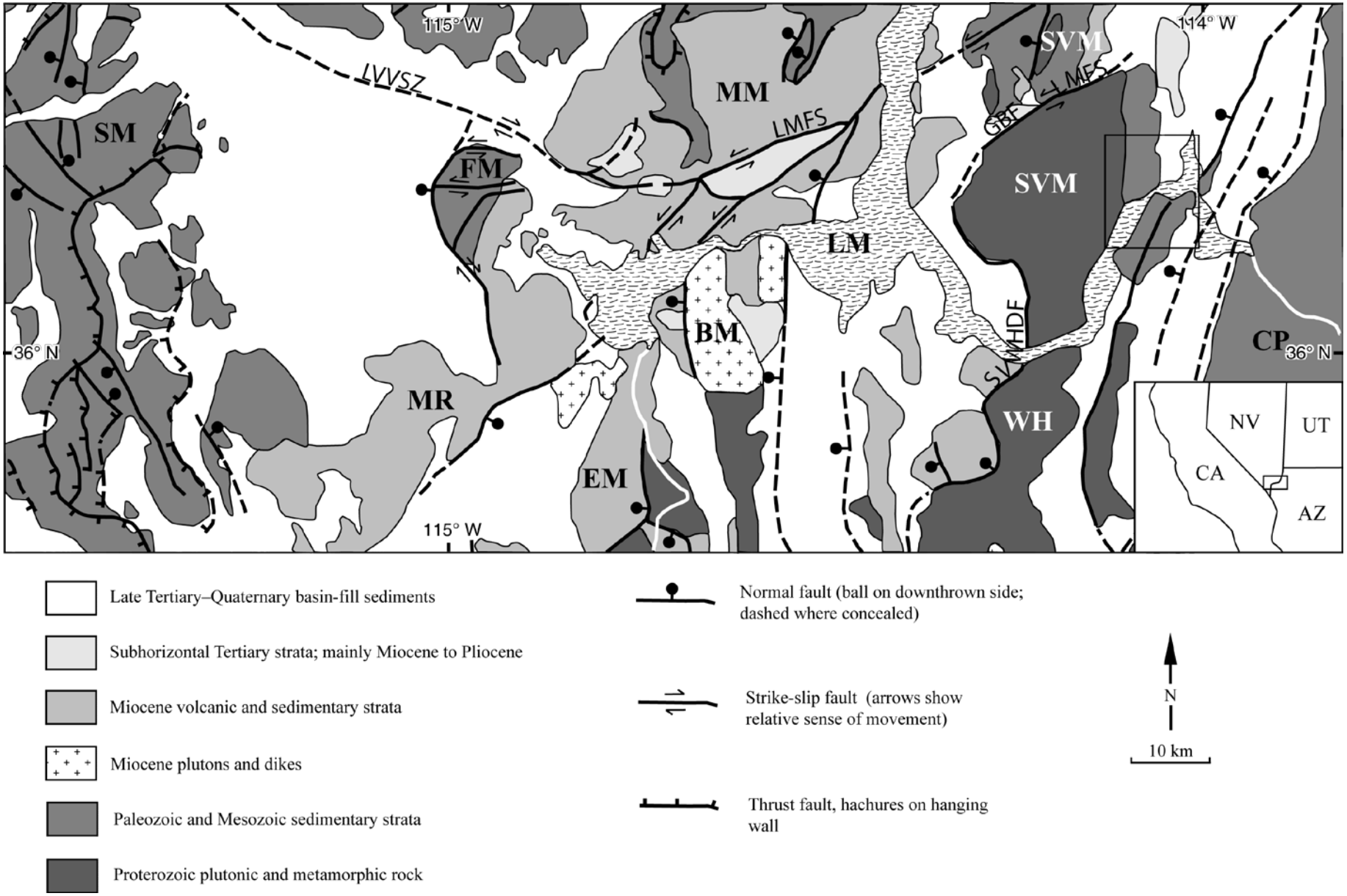

Figure 1. Generalized geologic map of the northernmost portion of the Colorado River extensional corridor; the Iceberg Canyon quadrangle is outlined by a black box. BM, Black Mountains; CP, Colorado Plateau; EM, Eldorado Mountains; FM, Frenchman Mountain; GBF, Gold Butte fault; LM, Lake Mead; LMFS, Lake Mead fault system; LVVSZ, Las Vegas Valley shear zone; MM, Muddy Mountains; MR, McCullough Range; SM, Spring Mountains; SVM, southern Virgin Mountains; SVWHDF, South Virgin–White Hills detachment fault; WH, White Hills. The white line indicates the Colorado River.

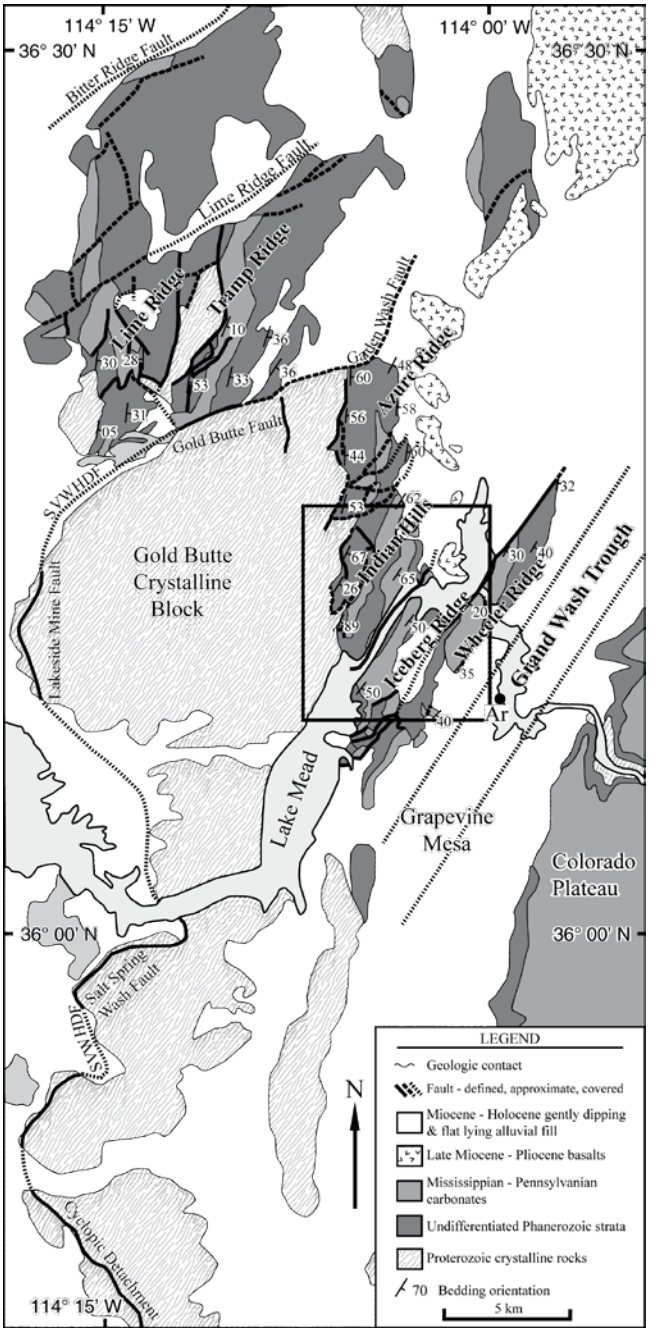

Figure 2. Simplified geologic map of part of the southern Virgin Mountains; the Iceberg Canyon quadrangle is outlined by a black box. The point labeled Ar represents the location of the newly dated tuff within unit Tsgw (see figure 4). SVWHDF, South Virgin–White Hills detachment fault.

In contrast to most of the Colorado River extensional corridor, this northeasternmost part is relatively amagmatic and is dominated by outcrops of metamorphic and sedimentary rocks. Neogene volcanism within the extensional corridor and north of Lake Mead is limited to the Miocene Hamblin–Cleopatra volcano west of Lake Mead and relatively low-volume Miocene to Pliocene basalt flows, including those found in the Grand Wash trough, Colorado River valley, and along the Gold Butte fault (figure 1).

Although the effects of Neogene extensional processes dominate the current crustal configuration of the map area and the surrounding portions of the northern Colorado River extensional corridor, the area also records previous contractional deformation events. Although not understood in detail, at least two intervals of folding are suggested by field evidence. These include isoclinal folding that accompanied or predated Paleoproterozoic peak metamorphism, and post-metamorphic Paleoproterozoic or Mesoproterozoic folding around axes that are now steeply plunging (Fryxell et al., 1992). These structures predate intrusion of the 1.45-Ga Gold Butte Granite (work of L.T. Silver *in* Stewart, 1980; Reiners et al., 2000).

The Iceberg Canyon quadrangle lies in the foreland to the Mesozoic Sevier thrust belt (Burchfiel et al., 1974), but related contractional deformation is not apparent in the rocks within the quadrangle. However, Mesozoic contractional structures are clearly expressed as a major thrust sheet ~30 km to the west in the Muddy Mountains (Longwell, 1949; Longwell et al., 1965; Bohannon, 1983).

STRATIGRAPHY AND LITHOLOGIC UNITS

Proterozoic Crystalline Basement Units

Crystalline basement within the map area is dominated by Paleoproterozoic metamorphic rocks assigned to the Mojave terrane (Karlstrom and Bowring, 1988). These rocks include large outcrops of orthogneiss (Xog) and garnet-bearing paragneiss (Xgn), as well as smaller outcrops of ultramafic rocks (Xum), granitic gneiss (Xgc, Xmgf), leucogranitic gneiss (Xlg), and amphibolite (Xmgf). All of these rock units are interpreted to have a metamorphic age of 1.7–1.8 Ga, based on K/Ar and Rb/Sr ages of 1.7 Ga from pegmatites within unit Xgn (Wasserburg and Lanphere, 1965) and Sm/Nd ages of 1.67–1.78 Ga from granitoid basement rocks exposed in the surrounding areas of southeastern California, northwestern Arizona, and southwestern Utah (Bennett and DePaolo, 1987). In addition, field relationships, including involvement of these rocks in folding that predates intrusion of the Mesoproterozoic Gold Butte Granite, support the interpretation that they are all of Paleoproterozoic age (Fryxell et al., 1992).

The 1.45-Ga Gold Butte Granite (Yg) crops out on the westernmost edge of the quadrangle; this outcrop is part of a large pluton, extending to the west, of distinctive rapakivi granite that forms about 30 percent of the basement outcrop within the southern Virgin Mountains (Volborth, 1962; Howard et al., 2003). This granite has been dated at 1.45 Ga using both U/Pb in zircon (work of L.T. Silver *in* Stewart, 1980), and U/Pb in titanite (Reiners et al., 2000). The Gold Butte Granite is noteworthy both because it is part of the suite of anorogenic granites that occur in a belt that extends from the southwestern United States northeast into eastern Canada (Silver et al., 1977; Anderson, 1983), and because its distinctive lithology permits unique correlations in

provenance studies of tectonically disrupted sedimentary deposits. The presence of this rock type in clasts in proximal Miocene deposits at Frenchman Mountain, Nevada, has been used to argue that the Frenchman Mountain block has been tectonically transported >60 km westward from the area of the southern Virgin Mountains (Rowland et al., 1990; Fryxell and Duebendorfer, 2005).

Paleozoic Stratigraphy

A 2.5- to 3-km-thick succession of Paleozoic sedimentary rocks, comprising two carbonate-dominated sequences, rests nonconformably on the crystalline basement complex within the Iceberg Canyon quadrangle (figure 3). The lower sequence is bounded on its base by the Proterozoic to lower Cambrian nonconformity. The two sequences are separated by the upper Cambrian to Devonian disconformity, and the top of the upper sequence is bounded by a middle Permian to Miocene unconformity. It is noteworthy that the middle Permian to Miocene unconformity results from the southward merging of the middle Permian to lower Triassic, basal Jurassic, and sub-Tertiary unconformities just to the north of the quadrangle. Triassic rocks crop out within a few hundred meters of the northern edge of the quadrangle and Jurassic rocks crop out ~5 km north of the quadrangle.

The basal Paleozoic sequence includes the lower Cambrian Tapeats Sandstone (Ꞓt) and overlying shales and limestone of the lower and middle Cambrian Bright Angel Shale (Ꞓb) (Noble, 1914; Schenk and Wheeler, 1942; Wheeler, 1943; McKee, 1945; Wheeler and Beesley, 1948); this succession is approximately 60 m thick, with significant variability due to tectonic thickening and thinning of the Bright Angel Shale. The basal Paleozoic sequence also includes an overlying carbonate-dominated succession, which is approximately 580 m thick on Wheeler Ridge. It is composed of the middle to upper Cambrian Muav Limestone ($Ꞓm_{1–2}$, $Ꞓm_{3–4}$, $Ꞓm_5$; Noble, 1914; McKee, 1945; Longwell, 1949; Longwell et al., 1965), only the lowest member ($Ꞓm_1$) of which is limestone; the remainder of the formation is dominantly dolostone in the map area.

The second sequence is composed of a sandwich of two carbonate-dominated successions that are separated by a siliciclastic succession. The lower carbonate succession is approximately 500–800 m thick, and is composed of an unnamed Devonian dolomitic sandstone and Devonian Sultan Limestone (mapped together as Ds; Hewett, 1931; McNair, 1951), the Mississippian Redwall Limestone (Mr; Gilbert, 1875; Hewett, 1931; Langenheim, 1963; McKee, 1963), the Pennsylvanian Callville Limestone (Pc_1, Pc_2; Longwell, 1921; McNair, 1951; Lumsden et al., 1973), and the Permian Pakoon Limestone (mapped with upper Callville Limestone, Pc_2; McNair, 1951; McKee, 1975; Billingsley, 1997). Although most of these units are named as limestones, the Devonian and Mississippian units are variably altered to dolostone in the Iceberg Canyon quadrangle. The middle siliciclastic succession has an average thickness of about 575 m and is composed entirely of Permian rocks (Darton, 1910; White, 1929; McKee, 1934, 1969, 1975; McNair, 1951; McKee, 1969; McKee, 1975; Billingsley, 1997). In ascending order, it consists of the Queantoweap Sandstone (Pq), the Hermit Formation, and the Coconino Sandstone (mapped together with the Hermit Formation, Pch). These units vary in thickness throughout the map area due to differences in primary depositional thickness as well as probable tectonic thickening and thinning, particularly within the incompetent mudstones and fine-grained sandstones of the Hermit Formation. The overlying upper succession of limestone is made up of the Permian Toroweap Formation (Pt) and Kaibab Limestone (Pk; middle Permian; McKee, 1938). It has a maximum thickness within the quadrangle of approximately 235 m and thins toward the southeast, reaching zero thickness directly south of Lake Mead.

Cenozoic Stratigraphy

Two sequences of Cenozoic strata are present; one lies disconformably on Paleozoic and Mesozoic strata and is tilted, the other is in angular unconformity on all older rocks and is more-or-less flat lying (figure 3).

The tilted sequence, although regionally present with thickness of as much as ~600 m (Brady et al., 2000), is represented within the Iceberg Canyon quadrangle by just two small outcrops, located ~1.5 km east of Iceberg Canyon. One of these is an exposure of an approximately 50-m-thick incomplete section of the conglomeratic Thumb Member of the Miocene Horse Spring Formation (Th) (Longwell, 1921; Bohannon, 1984; Beard, 1996). The other is a deposit of crackle breccia (Tbp) with an exposed thickness of ~20 m; it is located ~1 km south of the Th outcrop. The Thumb Member conglomerates and sandstone beds exhibit upsection fanning of dips from ~58° to 17°, consistent with the interpretation that the Thumb Member was deposited syntectonically during major extensional deformation (Beard, 1996). The crackle breccia deposit lies unconformably on the Callville Formation and is entirely composed of clasts derived from Paleozoic strata. It is interpreted as a rock avalanche deposit likely derived from fresh, steep fault scarps of the surrounding southern Virgin Mountains during or shortly after extensional deformation. It is therefore interpreted to be part of the lower, tilted sequence of Cenozoic strata and is likely of mid-Miocene age, equivalent in age to the Thumb Member. However, due to a lack of distinct bedding to constrain the degree of tilting, and no exposed relationship with other Miocene or Pliocene units, a younger age cannot be ruled out.

Above the tilted sequence is a sequence of siliciclastic rocks, basalt flows, and ash-fall tuffs that have been informally named the rocks of the Grand Wash trough (Lucchitta, 1966; Bohannon, 1984; Wallace et al., 2005). Within the Iceberg Canyon quadrangle, this sequence includes conglomerates, sandstones, and siltstones of middle Miocene to early Pliocene age that were deposited in local sub-basins partially separated by Wheeler Ridge (map units Tcg, Tsgw, Ttpf, Tcgw, Trgw).

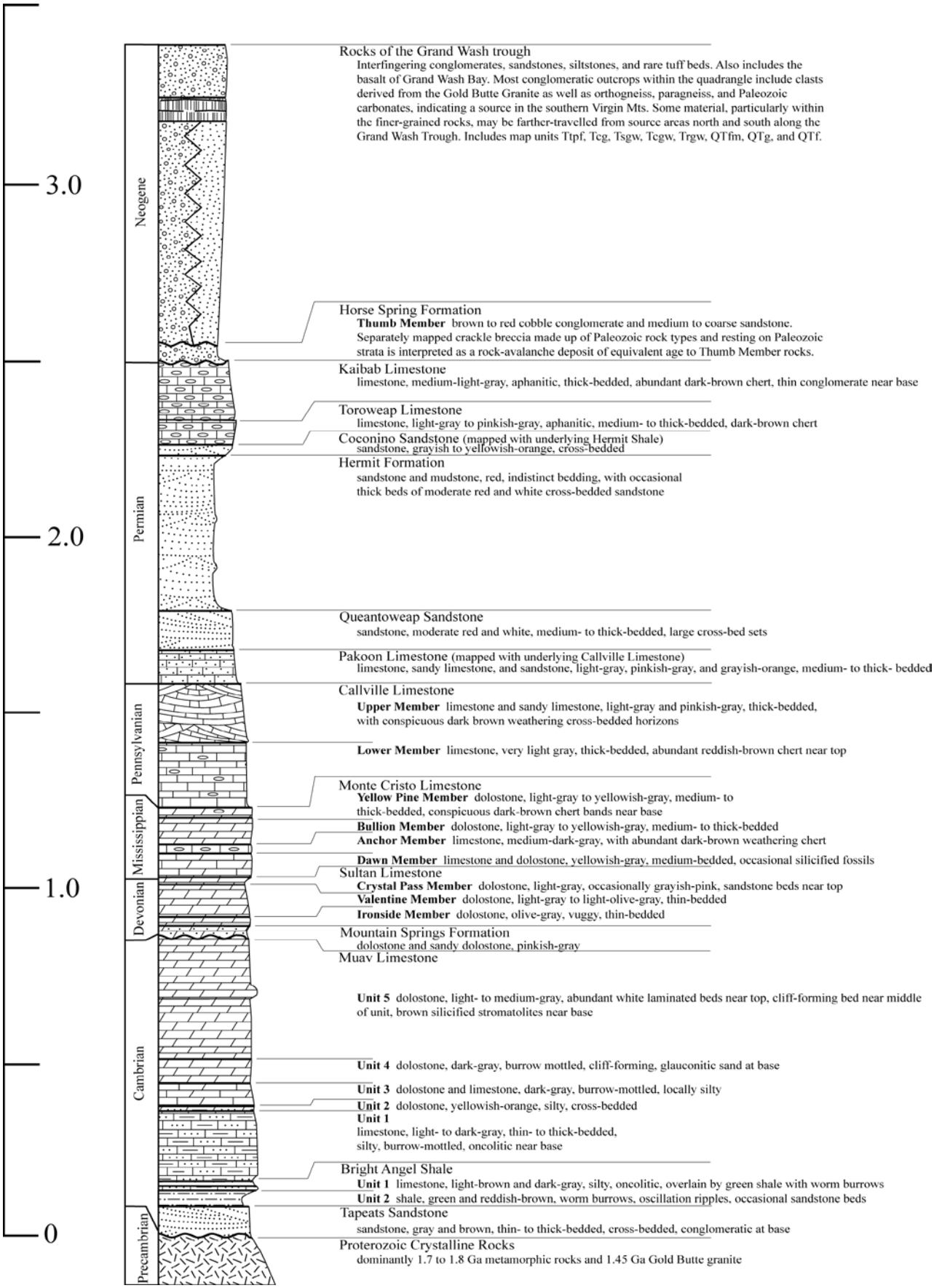

Figure 3. Simplified stratigraphic column for the Iceberg Canyon quadrangle. Scale bar shows thickness in kilometers. Thicknesses of units were calculated from 1:12,000-scale field maps.

Southeast of Wheeler Ridge, a >200-m-thick accumulation of conglomerate (Tcg; c.f. Wallace et al., 2005) forms a deeply incised alluvial fan that contains large (>5 m) coarsely porphyritic granite boulders derived from the Gold Butte Granite, indicating a sediment source farther west in the southern Virgin Mountains (Lucchitta, 1966; Lucchita and Young, 1986). Deposits of Tcg also form a thin finger that extends through a paleo-canyon that cuts across Wheeler Ridge and are found partially filling every significant valley between the Grand Wash trough and the Gold Butte Granite outcrops in the southern Virgin Mountains. This depositional pattern is consistent with interpretation of this unit as an alluvial fan that built eastward from the crystalline basement of the southern Virgin Mountains. The conglomerates of unit Tcg interfinger eastward with the sandstone and siltstone of unit Tsgw. At least four dated ash-fall tuffs are interbedded with the sandstone and siltstone unit. The lowest dated tuff occurs as a flat-lying layer in a conglomeratic interval within a small cove ~450 m east of the quadrangle; biotite phenocrysts from this tuff yielded an $^{40}Ar/^{39}Ar$ plateau age of 13.94±0.12 Ma (Isochron Age: 13.69±0.11 Ma; figure 4). The next stratigraphically higher tuff is the mapped tuff of Pearce Ferry (Ttpf), which has yielded an $^{40}Ar/^{39}Ar$ age of 13.11±0.08 Ma on sanidine (interpreted as a maximum eruptive age; Wallace et al., 2005). The two stratigraphically highest tuffs are mapped together as undifferentiated tephras (Ttu), and have yielded zircon fission track ages of 11.6±1.2 Ma and 11.1±1.3 Ma for the lower of the two tuffs and 10.8±0.8 Ma for the highest tuff (Bohannon, 1984).

Northwest of Wheeler Ridge, the rocks of the Grand Wash trough include both siliciclastic units and basalt flows. The stratigraphically lowest unit is the conglomerate of Grand Wash Bay (Tcgw), which is overlain by the red sandstone and siltstone of Grand Wash Bay (Trgw). Although deposited in a separate sub-basin, and differing in appearance due to a large matrix component of red sand and silt, Tcgw and Trgw are otherwise similar to, and may correlate in age with Tcg and Tsgw. The age of Tcgw and the base of Trgw are not directly constrained, but the upper part of Trgw interfingers with the basalt of Grand Wash Bay (Tbgw), which has yielded a K-Ar age of 3.8±0.11 Ma (Damon et al., 1978) and is probably part of the same eruptive sequence as the Sandy Point basalt in the adjacent Meadview North quadrangle ($^{40}Ar/^{39}Ar$ age: 4.41±0.03 Ma; Wallace et al., 2005). The observation that the upper part of Trgw interfingers with Tbgw, and must therefore be Pliocene in age, requires a modification of the earlier suggestion that this red sandstone and siltstone unit is entirely older and approximately correlative with the informally named red sandstone of White Basin and the Frenchman Mountain area in the western Lake Mead region; that unit has yielded ages of ~11.9–10.6 Ma (Bohannon, 1984). The lower part of Trgw and Tcgw may still correlate with the red sandstone unit in the western Lake Mead region (and with units Tcg and Tsgw).

The deeply eroded conglomerate (Tcg) and interfingering sandstone and siltstone deposits (Tsgw) are

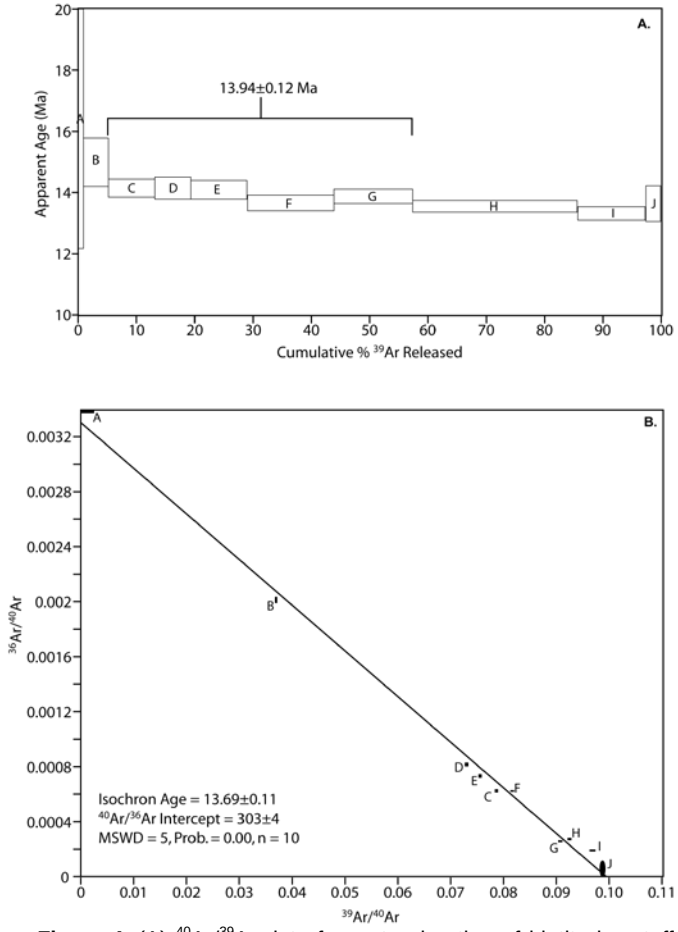

Figure 4. (A) $^{40}Ar/^{39}Ar$ data from step heating of biotite in a tuff interbedded with Tsgw. The sample was collected about 450 m east of the quadrangle boundary at 36° 08' 25.2"N, 113° 59' 41.8" W. Heating steps were run at 650°C, 750°C, 850°C, 920°C, 1000°C, 1075°C, 1110°C, 1180°C, 1210°C, and 1250°C, corresponding to A through J, respectively. A weighted mean plateau age of 13.94±0.12 Ma was determined from steps C to G. (B) Isochron plot yielding an age of 13.69±0.11 Ma.

overlain by at least three distinguishable generations of younger alluvium. These deposits include the pediment, stream, and alluvial fan deposits of Grapevine Wash (QTg), as well as younger alluvial fan and pediment deposits (Qf), and active alluvial channel and fan deposits (Qa).

Regionally, unconsolidated to weakly consolidated Colorado River gravels (QTcg) are found both overlying and underlying the basalt of Grand Wash Bay. However, within the Iceberg Canyon quadrangle, these gravels have been observed only as isolated erosional remnants on low hilltops and ridge crests east of Iceberg Canyon and west of Gregg Basin; these deposits rest unconformably on tilted Paleozoic strata, and their relationship to any dateable Cenozoic unit is unclear.

The deeply incised fanglomerate of Million Hills (QTfm) forms the eastern slope of Azure Ridge and the Indian Hills and was deposited as an alluvial fan, or a set of coalescing alluvial fans, that lap onto units Tcg, Tcgw, Trgw, and Tbgw. This incised alluvial fan deposit is overlain by at least three younger generations of alluvium, these being the Chemehuevi Formation (QTc; Longwell,

1936; Lucchitta, 1966), alluvial fan and pediment deposits of Grand Wash Bay (QTfgw), and active alluvial channel deposits (Qa).

Cross-bedded, poorly consolidated sandstone and siltstone of the Chemehuevi Formation (QTc; Longwell, 1936; Lucchitta, 1966) crops out in only one location: near the eastern edge of the quadrangle, north of Lake Mead and south of Cormorant Cliffs. Although this outcrop occurs as an isolated unit, resting disconformably on the fanglomerates of Million Hills (QTfm) and late to middle Miocene conglomerate (Tcg), it is known to grade laterally into deposits of Colorado River gravels (QTcg) farther to the south, within the Meadview North quadrangle.

In addition to the deposits discussed above, Quaternary alluvium (QTf, Qf, Qa), landslide deposits (QTl), and colluvium (Qc) occur as small deposits throughout the quadrangle. Detailed examination of these deposits suggests a complex history of deposition and incision, with individual drainages commonly containing two to four different levels of Quaternary alluvial terraces, but these terraces cannot easily be correlated from drainage to drainage and are mapped together as Qa.

STRUCTURE

Normal Faulting

The physiography of the Iceberg Canyon quadrangle is dominated by the effects of WNW–ESE-directed Miocene extension. Within the map area, there are five distinct topographic ridges, made up dominantly of resistant Paleozoic carbonate strata, each of which is a large normal-fault-bounded block. These ridges are, from east to west: Wheeler Ridge, Iceberg Ridge, the Indian Hills (making two ridges west of Iceberg Canyon), and Azure Ridge (figure 2). Each block is bounded on its east side by a west-side-down normal fault with >1 km of throw, and each is internally disrupted by smaller displacement, imbricate, dominantly west-dipping, west-side-down normal faults (cross section A–A'). The faults that bound the topographic ridges are, from east to west: the Grand Wash fault zone (in the subsurface directly east of the map area; Brady et al., 2000), the Wheeler Ridge fault, the Iceberg Canyon fault (Longwell, 1936, 1945), the Indian Hills fault, and the Million Hills Wash fault.

These major, top-to-the-west normal faults decrease in average dip from east to west, with the eastern faults dipping relatively steeply (~60–90°), and the western faults dipping very shallowly (~0–15°), but all cut bedding in their hanging walls at angles of 60–90°, suggesting originally steep dips. Hanging-wall cut-off angles tend to decrease downsection, suggesting that the faults originated with listric geometries (Brady et al., 2000). Locally, these major normal faults show significant variations in dip over short distances, perhaps due either to original complexity of the fault plane geometries or later folding.

The imbricate normal faults that internally disrupt each of the major fault blocks have accommodated smaller amounts of throw (typically a few meters to a few hundred meters), and dip steeper than, and typically merge downward into the main ridge-bounding faults. Only a few cases of these faults cross-cutting more shallowly dipping faults are observed within the Iceberg Canyon quadrangle, most notably in the southern portion of the Indian Hills, ~1 km north of Devil's Cove. These smaller-offset imbricate normal faults also cut bedding at higher angles than the main ridge-bounding faults, with hanging-wall cut-off angles as high as 124°, suggesting significant tilting of strata prior to initiation of these faults (c.f. Brady et al., 2000).

In addition to the top-to-the-west ridge-bounding faults and the smaller offset imbricate faults that merge into them, there are a few examples of steeply east-dipping to vertical, east-side-down faults within the quadrangle. These faults cut across all other faults, and therefore must have initiated later. They also decrease in both offset and abundance away from the main crystalline block on the west side of the quadrangle. The late, east-side down fault with the greatest offset is found along the boundary between the Paleozoic carbonate rocks and Proterozoic crystalline rocks on the west side of Azure Ridge, where it cuts out >100 m of Cambrian strata. Other examples of late, east-side down faults are found as bedding-plane-parallel faults that cut earlier west-side-down normal faults within Azure Ridge and the Indian Hills; these faults have throws of a few meters to tens of meters. No examples of late, east-side-down faults were observed east of Lake Mead.

Overall, normal faulting appears to have accommodated extension in a WNW–ESE direction, with hanging-wall blocks usually moving relatively WNW above a set of WNW-dipping normal faults. Although the normal faults within the map area form a complex, anastamosing map pattern, they have a fairly consistent average strike of ~212° and a consistent pattern of down-dip slip lineations (average dip direction of 301°; Brady et al., 2000). The five ridge-bounding normal faults apparently initiated first, probably cutting through nearly flat-lying strata in the foreland of the Sevier thrust belt (Burchfiel et al., 1974); they show no cross-cutting relationships with each other and all seem to cut bedding at similar angles, consistent with near-synchronous initiation of slip. The imbricate normal faults within each ridge block probably initiated later, consistent with their steeper average dips, higher hanging-wall cut-off angles, and observed downward merging with the ridge-bounding faults. Note that this commonly observed downward merging relationship requires that the ridge-bounding and later imbricate faults continued to slip synchronously. The last set of faults to initiate in the area were the east-side-down structures that, because of their steep dips and/or small throws, accommodated only minor extension. These faults may have primarily accommodated uplift of the crystalline block to the west of the quadrangle, western parts of which have been interpreted to have been unroofed from depths of ≥10 km (Fryxell et al., 1992; Reiners et al., 2000).

Folding

In addition to being affected by normal faulting, the rocks within the Iceberg Canyon quadrangle are strongly affected by fault-related folding. This folding is most easily seen within the Paleozoic strata, with rollover anticlines clearly visible in the hanging walls of the Iceberg Canyon fault, the Indian Hills fault, and the Grand Wash fault zone. These rollovers are expressed as a westward (or structurally upward) decrease in dip within each hanging-wall block. The rollover folds above the Iceberg Canyon fault and Grand Wash fault zone are particularly well known, as they are easily seen from Lake Mead (figure 5). In the hanging wall to the Iceberg Canyon fault, dips decrease from values as high as 66° at lake level on the western edge of Iceberg Canyon, down to 44° near the crest of the ridge only ~500 m west of the canyon. Similarly, the strata within Wheeler Ridge, above the Grand Wash fault zone, decrease in dip westward from values of 35–40° near lake level on the eastern side of the ridge down to average values of ~25° on the western edge of the ridge.

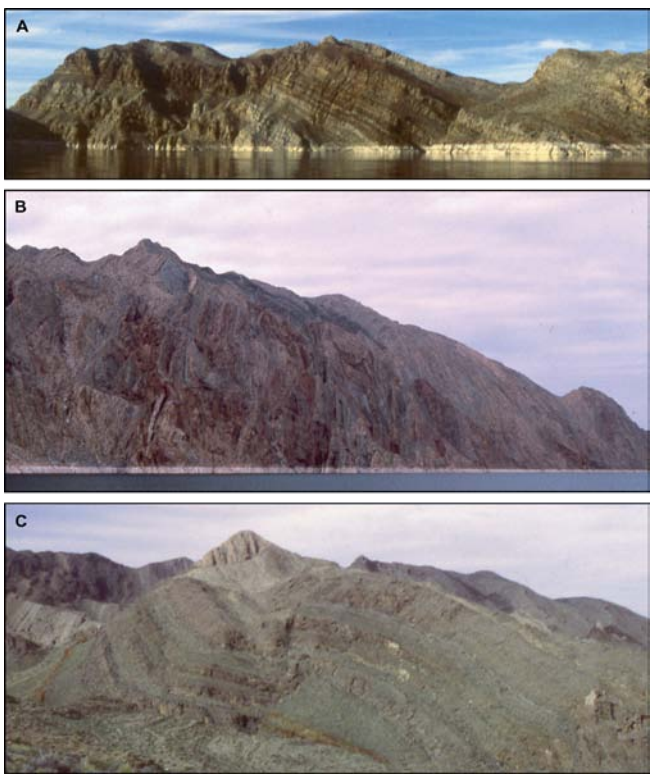

Figure 5. Photographs of the three largest rollover anticlines (reverse drag folds) within the Iceberg Canyon quadrangle. (A) Wheeler Ridge, as seen looking northward from Lake Mead, visible folded strata include units Mr, Pc_1, and Pc_2. This fold occurs above the buried Grand Wash fault zone. (B) The west side of Iceberg Canyon, as seen looking northward from Lake Mead, visible folded strata include Mr, Pc_1, and Pc_2. This fold occurs above the Iceberg Canyon fault, which is submerged about 40 m below lake level (Longwell, 1936). (C) Central portion of the Indian Hills as seen looking northward near 36° 12’ 16” N, 114° 05’ 32” W; visible folded strata include Cb, Cm_{1-2}, and Cm_{3-4}. This fold occurs immediately above the Indian Hills fault, which is not visible in this photograph, but is exposed at the base of the hill slope, about 30 m below the brown-weathering horizon (upper Cb) near the bottom-center portion of the image.

The rollover above the Indian Hills fault is less well known, as it cannot be seen from any easily accessible point, but it is the tightest of the three major rollover folds. An erosional window through the Indian Hills fault, centered at 36° 12’ 16” N, 114° 05’ 32” W, shows the fault to be approximately horizontal in this area, and Cambrian strata directly above it roll over very sharply, with dips decreasing from values as high as 86°E to only 10°E over an east–west distance of ~650 m (figure 5C).

All of the observed rollover folds are interpreted as being caused by collapse of the hanging wall strata into the potential void that is created by slip along listric normal faults (c.f. Hamblin, 1965; Dula, 1991). No detailed kinematic analysis of the folds within the Iceberg Canyon quadrangle has been carried out at this time, but the accessibility of these folds, combined with excellent exposure of bedrock, makes them prime candidates for testing of kinematic models of rollover formation.

TIMING OF DEFORMATION

The timing of deformation in the southern Virgin Mountains, including the Iceberg Canyon quadrangle, is constrained by a variety of cooling ages, both from samples of the Proterozoic crystalline basement and from volcanic units within the Cenozoic strata. The crystalline complex that crops out on the west side of the Iceberg Canyon quadrangle is part of an essentially structurally intact block that continues to the west, northwest, and southwest. It has been dated using K/Ar and Rb/Sr in feldspars (Wasserburg and Lanphere, 1965), U/Pb in zircon, monazite, apatite, and titanite (work of L.T. Silver *in* Stewart, 1980; Brady, 1998; Reiners et al., 2000), $^{207}Pb/^{206}Pb$ in zircon, titanite, and apatite (Reiners et al., 2000), apatite and zircon fission track (Parolini et al., 1981; Fitzgerald et al., 1991; Bernet et al., 2002), K/Ar in muscovite (Wasserburg and Lanphere, 1965), $^{40}Ar/^{39}Ar$ in muscovite (Brady, 1998; Reiners et al., 2000), and (U-Th)/He in apatite, sphene, and zircon (Reiners, 2002; Reiners et al., 2002). The large amount of cooling-age data for the rocks of the crystalline complex make it one of the thermochronologically best-studied areas in the world; although most of these ages come from rocks located west of the Iceberg Canyon quadrangle, they are all from what is interpreted to be a structurally continuous block and are therefore relevant to interpreting the timing of deformation within the quadrangle.

The timing of deformation is further constrained by absolute dating of both the tilted and untilted Cenozoic strata that crop out within the quadrangle and elsewhere in the Lake Mead region. The available dates within the Cenozoic section consist of previously published K/Ar, $^{40}Ar/^{39}Ar$, and fission track dates for basalts and tuffs (Anderson et al., 1972; Bohannon, 1984; Damon et al., 1978; Shafiqullah et al., 1980; Carpenter et al., 1989; Cole, 1989; Beard, 1996), as well as a new $^{40}Ar/^{39}Ar$ age from a tuff interbedded with unit Tsgw (figures 2, 4).

Although a detailed presentation of all above-mentioned thermochronologic data is beyond the scope of

this manuscript, the implications of those data for timing of deformation will be discussed below. The thermochronologic data set records cooling ages that are coincident with at least five periods of significant deformation and/or thermal perturbation, including Paleoproterozoic compressional deformation and metamorphism, Mesoproterozoic igneous intrusion, Cretaceous thrust faulting, localized late Cretaceous to Paleocene igneous intrusion, and Miocene (to possibly Holocene) extension.

Pre-Cenozoic deformation of the area is incompletely understood because these events are recorded in the crystalline basement rocks, which have not been studied in detail, and in Mesozoic foreland basin deposits, which are not present in the area and have presumably been erosionally removed. Nevertheless, the thermochronologic data provide a record of the general timing of the pre-Cenozoic deformational events. The Paleoproterozoic (~1.7–1.8 Ga) metamorphic event is recorded by K/Ar and Rb/Sr ages from pegmatites within the crystalline block to the west of the quadrangle (Wasserburg and Lanphere, 1965). Mesoproterozoic (1.45 Ga) intrusion of the Gold Butte Granite is recorded by U/Pb zircon and titanite ages within the intrusion (work of L.T. Silver *in* Stewart, 1980; Reiners et al., 2000), and by reset K/Ar and $^{40}Ar/^{39}Ar$ ages in the adjacent gneisses (Wasserburg and Lanphere, 1965; Brady, 1998). Late Cretaceous thrusting and/or magmatism that is known to the west of the area may be reflected in $^{40}Ar/^{39}Ar$ muscovite cooling ages of ~90 Ma (Brady, 1998; Reiners et al., 2000). Finally, a latest Cretaceous or earliest Paleocene intrusive event is recorded by a U/Pb in monazite age of 65.2±0.6 Ma from the muscovite-biotite granite that crops out 13.5 km west of the quadrangle in the southwestern portion of the southern Virgin Mountains (Brady, 1998).

The timing of Cenozoic extensional deformation is better constrained, due to abundant relevant thermochronological data from the basement rocks, and to dated syn- and post-deformational Cenozoic strata. Early, small magnitude extension and localized normal faulting probably occurred as early as ~24–25 Ma, because an upward decrease in dips (i.e. growth-fault fan) occurs within the basal conglomerate of the Rainbow Gardens Member of the Horse Spring Formation in Pigeon Wash near the north end of Wheeler Ridge (Brady, 1998). This outcrop is ~3.5 km east of the Iceberg Canyon quadrangle, and is deposited on Paleozoic carbonates that are structurally continuous with those that crop out near the eastern edge of the quadrangle. The basal conglomerate in the outcrop at the north end of Wheeler Ridge is probably slightly older than the 24±0.1 Ma age that has been determined from a tuff collected 70 m above the base of the Rainbow Gardens Member elsewhere in the Lake Mead area (Bohannon, 1992).

The interpretation of early, small magnitude extension at the time of onset of deposition of the Rainbow Gardens Member is also consistent with the overall distribution of the Rainbow Gardens Member, the middle and upper parts of which are dominated by limestone that was apparently deposited in a closed, broad shallow basin (Beard, 1996). One reasonable explanation for the origin of such a basin is early extensional thinning and subsidence of the crust. However, the Rainbow Gardens Member generally dips concordantly with underlying Paleozoic and Mesozoic strata, requiring that it predates major extensional deformation and tilting in the area.

Rapid, large-magnitude extension is interpreted to have begun at ~16 Ma, and continued for probably less than 2 Ma. Both apatite fission-track and apatite (U-Th)/He cooling ages from across the crystalline block to the west of the Iceberg Canyon quadrangle record cooling ages that fall in the range of 14–17 Ma (mean age: 15.5 Ma) for samples that were interpreted as being fully reset prior to Basin and Range extension (Fitzgerald et al., 1991; Reiners et al., 2000). The onset of rapid extension is also recorded by development of a disconformity in the Horse Spring Formation, which may represent erosional removal of ~2.5 Ma of stratigraphic record between the Rainbow Gardens Member (≥26 Ma to ≤18.8 Ma; Beard, 1996) and the overlying Thumb Member (≥16.2 Ma to ≤14.2 Ma; Beard, 1996). The development of significant fault scarps is interpreted to be recorded by the occurrence of landslide megabreccia deposits in the Thumb Member. The age of these deposits is poorly constrained for most outcrops, but one example north of the Lime Ridge fault (figure 2) occurs ~20 m below a tuff dated at 14.2±0.5 Ma (Beard, 1996), requiring the generation of significant topographic relief by that time. The generation of significant topographic relief and tectonic unroofing of the crystalline basement within the southern Virgin Mountains during middle Miocene time is also suggested by the occurrence of coarse conglomerates north of the Gold Butte fault (figure 2), which contain clasts of Proterozoic rocks eroded from the southern Virgin Mountains and are overlain by a tuff dated at 14.4±0.3 Ma (Beard, 1996). Although there is evidence of fault scarp development and complex depositional patterns in the lower part of the Thumb Member, significant up-section decreases in dip, indicative of horizontal axis rotation of fault blocks, are seen only within the upper alluvial-fan dominated part of the section. The lowest dated tuff from this upper part of the section yields an age of 14.4±0.5 Ma (Beard, 1996). The period of significant horizontal axis rotation (i.e. tilting), which could reasonably be interpreted as the period of most rapid extension, apparently only persisted for ~0.5 Ma, as the lowest dated tuff interbedded with the flat-lying sandstone and siltstone of Grapevine Wash (Tsgw) yields a $^{40}Ar/^{39}Ar$ in biotite plateau age of 13.94±0.12 Ma (Isochron age: 13.69±0.11 Ma; figure 4). Relevant data can also be found in Duebendorfer and Sharp (1998), Faulds et al. (2001a,b), and Wallace et al. (2005).

Extensional deformation since that time has been relatively minor, as the rocks of the Grand Wash Trough are still generally flat-lying. However, monoclinal warping of the upper Miocene Hualapai Limestone and Pliocene Colorado River gravels in the hanging wall of the Wheeler Ridge fault suggest ~400 m of west-side-down throw across the fault since ~6 Ma (Howard et al., 2000). In addition, unconsolidated alluvium of unknown age (Pleistocene to

possibly Holocene) is faulted in a number of locations along the western flank of the southern Virgin Mountains, suggesting the possibility that minor extension has continued to Holocene time.

CONCLUSIONS

The Iceberg Canyon quadrangle is located in the northernmost portion of the northern Colorado River extensional corridor at the eastern edge of the central Basin and Range province. The quadrangle includes the immediate hanging wall of the Grand Wash fault zone, which defines the eastern structural boundary of the central Basin and Range. It also includes part of the footwall of the South Virgin–White Hills detachment fault, which is the easternmost large-offset extensional detachment in the central Basin and Range. This footwall block is a more-or-less intact slice of upper crust that is probably ≥10 km thick. The quadrangle includes Proterozoic crystalline basement, overlain by a carbonate-dominated Paleozoic sedimentary sequence and a clastic-dominated Cenozoic sedimentary sequence.

The rocks within the quadrangle record rapid, large-magnitude mid-Miocene extension, which was nearly complete by ~13.9 Ma. Extension was primarily accommodated on a set of subparallel, initially steeply to moderately west-dipping listric normal faults. The hanging walls to each of these major faults was broken by dominantly west-dipping, smaller-offset, imbricate normal faults that initiated after some amount of slip and rotation of the first-generation fault set. These later faults typically sole into the earlier-formed faults. Due to a combination of domino-style rotation, translation down listric fault planes, and syn- to post-extensional isostatic rebound, the originally steeply to moderately dipping faults now have moderate to shallow dips. A third generation of steeply dipping, east-side-down faults also affects the area; these faults decrease in both abundance and offset away from the crystalline block that forms the footwall of the South Virgin–White Hills detachment, and they are interpreted here to be late-stage isostatic rebound accommodation features.

UNIT DESCRIPTIONS

Qa Alluvial deposits (Holocene) Gray to light-brown or light-reddish-brown, unconsolidated, poorly sorted and subround to angular gravel, pebbles, sand, and silt. Thin- (~3 cm) to medium-bedded. Incised into all older rock units; variable thickness up to ~10 m.

Qf Alluvial fan and pediment deposits (Holocene to late Pleistocene?) Gray to brown poorly consolidated, poorly sorted subangular to angular pebble to cobble, clast-supported conglomerate with subordinate lenses and thin beds of matrix-supported pebble and cobble conglomerate and coarse-grained sandstone. Clasts are locally derived, commonly from dissected older conglomerate (QTfgw, QTf, QTg, QTfm, QTcg, Tcgw, and Tcg). Bedding ranges up to 1.5 m thick. On steeper slopes, uppermost beds are overlain by minor colluvium. Probably post-extensional because the deposits cover exposures of the Grand Wash (not on this quad) and Wheeler Ridge faults. Up to 15(?) m thick.

Qc Colluvium (Holocene to Pleistocene?) Gray to light-brown, usually unconsolidated, rarely calcite cemented, poorly sorted, subangular to angular, boulder to sand. Although occurring on many slopes, this unit was mapped only where it was thick enough to conceal the underlying unit.

QTfgw Alluvial fan and pediment deposits of Grand Wash Bay (Holocene to Pleistocene?) Gray to brown, poorly sorted, poorly to moderately consolidated, subangular to angular pebble to cobble clast-supported conglomerate with medium- to coarse-grained sand matrix and subordinate lenses and beds of coarse-grained sandstone; clast composition suggests derivation from QTfm, Tbgw, Trgw, Tcgw, and Tcg. Occurs as slightly to strongly dissected erosional remnants adjacent to Grand Wash Bay, as much as 5 m higher than nearby Qa. Exposed thickness ~5 m.

QTl Landslide and talus deposits (Holocene to Pliocene?) Slump blocks and unconsolidated rubbly debris composed of angular cobbles and boulders of local bedrock; blocks range up to ~50 m in length and are up to ~10 m thick.

QTf Older alluvial fan and pediment deposits (Pleistocene to Pliocene?) Gray to brown, poorly sorted, poorly to moderately consolidated, subangular to angular pebble to cobble clast-supported conglomerate with medium- to coarse-grained sand matrix and subordinate lenses and beds of coarse-grained sandstone; beds generally up to 2 m thick; lithologically similar to Qf with clasts locally derived, commonly from dissected older conglomerate (QTg, QTfm, QTcg, Tcgw, and Tcg). Occurs as slightly to strongly dissected erosional remnants as much as 3 m higher than nearby Qf and Qa. Some upper surfaces contain clasts with rock varnish and thin caliche crusts suggesting relatively long exposure. Up to 15(?) m thick.

QTg Pediment, stream, and alluvial fan deposits of Grapevine Wash (Pleistocene to Pliocene?) Unconsolidated to poorly consolidated, moderately to subrounded, poorly sorted pebble to cobble clast-supported conglomerate and subordinate sandstone lenses and beds. Clast types indicate derivation from Tcg and exposed Paleozoic units in Wheeler Ridge, they range in diameter from a few mm to 0.75 m and include varnished basalt, granite, and Paleozoic limestone, chert, and sandstone. Medium- to coarse-grained sand matrix. Exposed as a thin veneer (≤10 m thick) in the southeast corner of the quadrangle.

QTfm Fanglomerate of Million Hills (Pleistocene to Pliocene?) Weakly to moderately indurated, medium to thick beds of poorly sorted, moderately rounded to subangular clast-supported conglomerate containing a coarse-grained sand matrix cemented by calcite; clast types include abundant Proterozoic gneiss and granite, as well as Paleozoic limestone, chert, and sandstone. Crops out as a deeply incised alluvial fan surface throughout the Million Hills, between Grand Wash Bay and Azure Ridge; laps onto Tbgw, indicating a Pliocene or younger age. Exposed thickness as much as ~40 m.

QTc Chemehuevi Formation (Pleistocene to Pliocene) The Chemehuevi Formation (Longwell, 1936) is a light-tan or buff, poorly consolidated to unconsolidated, moderately to well-sorted, rounded to subrounded medium- to coarse-grained quartz arenite and siltstone with common medium-scale cross-bedding. Within the Meadview North quadrangle to the south, QTc grades laterally into QTcg (Wallace et al., 2005). Exposed thickness ~25 m.

QTcg Colorado River gravels (Pleistocene to Pliocene) Unconsolidated to weakly consolidated, moderately to well-sorted, clast-supported conglomerate. Clasts are composed of well rounded to rounded pebbles and cobbles (1.5–20 cm in length) of resistant Paleozoic limestone, chert, fine-grained sandstone/quartzite (each ~30 percent), and ~10 percent Proterozoic granite, gneiss and pegmatitic quartz. Matrix consists of fine to coarse sand. Clasts are commonly coated with rock varnish. Crops out only as erosional remnants (mostly <2 m thick) exposed on tops of small hills near Lake Mead.

Tbgw Basalt of Grand Wash Bay (early Pliocene) Porphyritic olivine basalt; columnar jointed with spacing ranging from ~20 cm at the top to ~50 cm at the base; layering suggests at least 3 flows in the vicinity of Cormorant Cove; overlain by QTf, QTfgw, and QTfm; intercalated with Trgw. The basalt has yielded a 3.8±0.11 Ma K/Ar age (Damon et al., 1978) and has been correlated to the Sandy Point basalt (Lucchitta, 1966), which yielded an $^{40}Ar/^{39}Ar$ age of 4.41±0.03 Ma (whole rock) (Wallace et al., 2005). Total thickness ~60 m.

Trgw Red sandstone and siltstone of Grand Wash Bay (early Pliocene to middle Miocene?) Red, poorly to moderately consolidated sandstone and siltstone. Alternating beds of fine- to medium-grained sandstone, siltstone, and mudstone with subordinate lenses and minor interbeds of pebble conglomerate with coarse sand matrix; clasts mostly composed of granite or individual angular to subrounded grains of quartz, feldspar, and mafic minerals, clasts of basalt locally abundant; lenses of primary and/or secondary(?) gypsum locally common with individual laths 1–2 cm in length oriented perpendicular to bedding. This unit was previously included in the sandstone and siltstone facies of the Muddy Creek Formation (Longwell, 1936) and Muddy Creek Complex (Lucchitta, 1966), and the red sandstone unit of the rocks of the Grand Wash trough (Bohannon, 1984). Trgw is intercalated with Tbgw, suggesting an early Pliocene age for its top, the age of the base of the unit is unknown; this unit is possibly correlative in part with Tsgw. Maximum exposed thickness ~90 m.

Tcgw Conglomerate of Grand Wash Bay (early Pliocene to middle Miocene?) Medium grayish-red, poorly to moderately consolidated conglomerate and sandstone. Alternating beds of medium- to coarse-grained sandstone and pebble to cobble conglomerate with coarse sand matrix; clasts mostly composed of granite or individual angular to subrounded grains of quartz, feldspar, and mafic minerals, with lesser amounts of Paleozoic carbonate and sandstone. Crops out underneath Trgw on the west side of Grand Wash Bay; it is unclear whether this represents the base of Trgw, or a coarse-grained bed intercalated with Trgw; this unit is possibly correlative with Tsgw and/or Tcg. Maximum exposed thickness ~20 m.

Tsgw Sandstone and siltstone of the Grand Wash trough (late to middle Miocene) Red to gray and brown poorly to moderately consolidated sandstone and siltstone. Alternating beds of fine- to medium-grained sandstone, siltstone, and mudstone with subordinate lenses and minor interbeds of pebble conglomerate with coarse sand matrix; clasts mostly composed of granite or individual angular to subrounded grains of quartz, feldspar, and mafic minerals; root/stem traces and burrowing are common; lenses of primary and/or secondary(?) gypsum locally common with individual laths 1–2 cm in length oriented perpendicular to bedding. This unit was previously named the sandstone and siltstone facies of the Muddy Creek Formation (Longwell, 1936) and Muddy Creek Complex (Lucchitta, 1966), and was included in the red sandstone unit of the rocks of the Grand Wash trough (Bohannon, 1984). The unit ranges in age from <11 Ma to ≥14 Ma. Nonwelded ash-fall tuffs in the Pearce Ferry area intercalated within Tsgw yielded zircon fission track ages of 10.8±0.8 Ma to 11.6±1.2 Ma (Ttu; Bohannon, 1984) and an $^{40}Ar/^{39}Ar$ age of 13.11±0.08 Ma on sanidine (Ttpf; Wallace et al., 2005). Another nonwelded ash-fall tuff was found intercalated within Tsgw, near lake level, ~2 km north of Pearce Ferry and just east of the edge of the quadrangle, and was dated at 13.94±0.12 Ma (plateau age, $^{40}Ar/^{39}Ar$; step-heating experiment; isochron age: 13.69±0.11 Ma). Tsgw crops out in the southeast corner of the quadrangle, east of Wheeler Ridge, where it interfingers westward with Tcg. Tsgw could be sourced from the southern Virgin Mountains to the west, the Lost Basin Range or Garnet Mountain to the south, or a paleo-Colorado or Virgin River flowing from the north and/or east. Exposed thickness is as much as ~120 m; probably was much more extensive before erosion by the modern-day Colorado River.

Tcg Conglomerate (late to middle Miocene) Previously called Gregg's breccia by Lee (1908), the conglomerate and breccia units of the Muddy Creek Formation (Longwell, 1936), and conglomerate-breccia facies of the Muddy Creek Complex (Lucchitta, 1966). Brown, pinkish, and light-gray

poorly sorted, moderately to poorly consolidated conglomerate. The matrix of the conglomerate and interbedded lenses of sandstone consist of coarse- to medium-grained, poorly to moderately sorted, subangular grains of quartz, feldspars, and micas. Angular to subangular clasts in the conglomerate range in size from pebbles to large boulders (>5 m). Bedding thickness ranges up to ~2 m; includes both matrix and clast-supported beds; weakly to moderately cemented by calcite. Grades laterally into and interfingers with overlying sandstone/siltstone facies (Tsgw). Clasts derived from the ~1.45 Ga Gold Butte Granite and pebble imbrication indicate provenance from the Gold Butte block in the southern Virgin Mountains 6–15 km to the west (Lucchitta, 1966). The clasts derived from the Gold Butte Granite consist of a rapakivi-type granite and are coarsely porphyritic, euhedral to subhedral perthite biotite granite with a medium- to coarse-grained groundmass of potash feldspar, quartz, plagioclase, and biotite. The perthite is mantled by oligoclase and albite and clumps of biotite aggregates. Within the quadrangle, Tcg crops out along the west flank of Gregg Basin, in the valley west of Wheeler Ridge, and in the southeastern corner of the quadrangle as a deeply incised alluvial fan, which was apparently sourced from the South Virgin Mountains to the west, and built eastward through a paleo-canyon that cuts through Wheeler Ridge. Maximum exposed thickness is ~250 m.

Ttu Tephras, undifferentiated (middle Miocene) Two horizons of white to blue-gray very fine- to fine-grained nonwelded ash-fall tuff, intercalated within Tsgw a few meters stratigraphically above Ttpf in the Pearce Ferry area. Thicknesses of these tuffs range from ~30 to 50 cm. The lower of the two tuffs has yielded zircon fission track ages of 11.6±1.2 Ma and 11.1±1.3 Ma, and the higher tuff yielded a zircon fission track age of 10.8±0.8 Ma (Bohannon, 1984).

Ttpf Tephra in Pearce Ferry area (middle Miocene) White fine to medium-grained nonwelded biotite tuff with laminations consisting of 1 to 10 mm of brown mud. Contains ~5 percent phenocrysts of which ~40 percent are quartz, ~30 percent plagioclase, ~20 percent sanidine, and ~10 percent greenish-brown biotite. Groundmass consists of volcanic glass shards (~100–250 µm in length) preferentially oriented parallel to bedding). This tuff is intercalated with Tsgw near or at the shore of Lake Mead in the Pearce Ferry area. Thickness is ~0.5 to 2 m.

Tbp Crackle breccia (late to middle Miocene) Reddish-brown and gray, moderately to well indurated clast-supported crackle breccia; lithologies are entirely composed of Paleozoic strata. Tbp is deposited disconformably on Paleozoic strata. Tbp probably originated as rock-avalanche deposits derived from the steep slopes of the southern Virgin Mountains. Maximum exposed thickness ~20 m.

Th Thumb Member of the Horse Spring Formation (middle Miocene) Brown to red cobble conglomerate and medium- to coarse-grained sandstone; beds 10 to 50 cm thick; well indurated. Clasts include Paleozoic carbonates and sandstones, and Proterozoic gneiss and granite. This unit crops out along the wash that cuts through the ridge east of Iceberg Canyon. Its base is disconformable with the underlying Pakoon Limestone (Pc2); bedding dips fan upsection, decreasing from ~58° E to ~17° E through ~100 m of exposed section. Such rapid fanning of dips is typical of the syntectonic Thumb member of the Horse Spring Formation (Bohannon, 1984; Beard, 1996).

Pk Kaibab Limestone (Permian) Thick- to medium-bedded, cliff-forming, medium-light-gray, aphanitic limestone with abundant dark-brown chert stringers and nodules (fossiliferous). Basal bed is a thin (~1–2 m), red, cobble conglomerate, composed of clasts derived from Pc1 and Pc2, in a matrix of medium to coarse red sand; this bed is very recessive and rarely exposed. Total thickness ~150 m.

Pt Toroweap Formation (Permian) Thick- to medium-bedded, cliff-forming, light-gray to pinkish-gray, aphanitic limestone, includes dark-brown chert stringers and nodules (fossiliferous); distinguishable from Pk primarily by difference in color and less abundant chert. Total thickness ~85 m.

Pch Coconino Sandstone and Hermit Formation (Permian) The Coconino sandstone is grayish-yellow to orange, medium-grained, cross-bedded sandstone, ~10 m thick; typically forms a cliff above the Hermit Formation. The Hermit Formation is red, fine-grained sandstone and mudstone; bedding generally indistinct, with several thick (~2 m) beds of red and white cross-bedded, medium-grained sandstone. Total thickness ~475 m.

Pq Queantoweap Sandstone (Permian) Medium to thick bedded, moderate red and white, medium-grained, cross-bedded sandstone. Total thickness ~110 m.

Pc_2 Pakoon Limestone (Permian) and upper member of the Callville Limestone (Pennsylvanian) Thick- to medium-bedded, slope-forming, light-gray limestone and pinkish-gray sandy limestone; includes a few beds of yellowish-gray sandy limestone. Upper ~30 m is equivalent to the Pakoon Limestone (c.f. Billingsley, 1997). Basal bed is cross-bedded sandy limestone ~2 m thick that usually weathers to form a conspicuous dark-brown horizon. Total thickness ~100 m.

Pc_1 Lower member of the Callville Limestone (Pennsylvanian) Thick-bedded, slope-forming, very light-gray limestone. Abundant orange to reddish-brown chert stringers occur near the top of the unit. Total thickness ~150 m.

Mr Redwall Limestone (Mississippian) Thickly bedded yellowish-gray limestone and dolostone overlain by a conspicuous horizon of interbedded gray dolostone and dark-brown chert, generally fossiliferous, in turn overlain by medium-bedded light-gray to yellowish-gray sucrosic dolostone. This formation is a very prominent cliff-former,

commonly holding up ridge crests in the area. Total thickness is ~150 m.

Ds Sultan Limestone and unnamed sandstone (middle Devonian) The Sultan Limestone is a prominent cliff-forming olive-gray dolostone, commonly including abundant silicified stromatolites or vugs, overlain by less resistant, well-bedded olive-gray to light-gray dolostone. Well sorted, well-rounded pale pink to white quartz arenite beds or pinkish-gray sandy dolostone beds (total thickness ≤2 m) are locally found below the olive-gray dolostone. An outcrop of these unnamed sandstone beds farther to the north, on South Virgin Peak Ridge, yielded fish plate fossils identified as Holonema, Asterolepis and "crossopterygians" of middle Devonian age (Elliott and Johnson, 1997). Total thickness is ~140 m.

Ꞓm_5 Muav Limestone, unit 5 (late Cambrian) Equivalent to the upper part of the Banded Mountain Member of the Bonanza King Formation, although the beds equivalent to the uppermost Banded Mountain Member have been erosionally removed by the sub-Devonian unconformity. Prominent bench of light-gray, burrow-mottled dolostone overlain by medium-gray burrow-mottled dolostone and interbeds of light-gray to white cryptalgal dolostone. Total thickness is ~300 m.

Ꞓ$m_{3–4}$ Muav Limestone, units 3 and 4 (middle to late Cambrian) Equivalent to the lower part of the Banded Mountain Member of the Bonanza King Formation. Unit 3 is a dark-gray, cliff-forming, burrow-mottled dolostone with some orange overprint on silt-rich portions. Unit 4 is slightly less resistant, dark- to medium-gray dolostone with interbeds of light-gray to white cryptalgal dolostone. A prominent horizon of brown chert lenses occurs ~10 m above the base of unit 4. Total thickness is ~80 m.

Ꞓ$m_{1–2}$ Muav Limestone, units 1 and 2 (middle Cambrian) Equivalent to the Papoose Lake Member of the Bonanza King Formation. Prominent cliff-forming light-gray limestone overlain by medium-gray, bedded, burrow-mottled limestone and dolostone with an orange overprint, particularly on silt-rich burrows and along some bedding planes. The top of unit 2 is marked by a recessive orange-buff, cross-bedded carbonate grainstone. Total thickness is ~200 m.

Ꞓb Bright Angel Shale (middle Cambrian) Shale and subordinate limestone. The basal parts consist of green and reddish-brown shale containing worm burrows, oscillation ripples, and local cross-beds. The upper part consists of a light-brown and dark-gray oncolitic silty limestone, which is overlain by green shale with worm burrows. Approximate thickness ranges from 10 to 60 m.

Ꞓt Tapeats Sandstone (lower Cambrian) Highly indurated pale-brown to pale-reddish-brown thin- to thick-bedded, locally cross-bedded fine- to coarse-grained sandstone; includes both silica and calcite cement. Unconformably overlies early Proterozoic metamorphic rocks. Thickness ranges from 20 to 40 m.

pꞒu Undivided Proterozoic crystalline rocks (Proterozoic) Shown only in cross section.

Yg Gold Butte Granite (Mesoproterozoic) Named by Longwell (1936). Described by Volborth (1962). Coarse porphyritic perthite-quartz-biotite granite or biotite rapakivi granite, light-gray, weathering to light-brownish-gray. This rock is distinctive because of abundant euhedral and ovoid perthite phenocrysts commonly 1–3 cm long, and 0.5–2 cm wide, with some phenocrysts as long as 5 cm (Volborth, 1962); within the map area these large feldspar phenocrysts generally compose >50 percent of the rock by volume, but both abundance and size of crystals decreases westward (Fryxell et al., 1992). Locally the perthite phenocrysts are rimmed with oligoclase and albite (rapakivi texture). Average modal analysis (Volborth, 1962): 45.5 percent perthite, 27.2 percent quartz, 17.6 percent plagioclase, 6.2 percent biotite, 1.2 percent sphene, 0.75 percent chlorite (altered hornblende), 1.1 percent fluorite, oxides, apatite, and 0.45 percent allanite. The Gold Butte granite has yielded U-Pb zircon and titanite ages of 1.45 Ga (work of L.T. Silver in Stewart, 1980; Reiners et al., 2000).

Xlg Leucogranite gneiss (Paleoproterozoic) Weakly to moderately foliated fine- to medium-grained gneiss, equigranular to coarsely pegmatitic, light-gray to pink, except where altered to red directly under the sub-Cambrian nonconformity; composed of quartz, potassium feldspar, plagioclase, and less than 5 percent biotite. Includes rare garnet phenocrysts (xenocrysts?). Equivalent to the microcline granite of Volborth (1962).

Xmgf Granitic gneiss and amphibolite (Paleoproterozoic) Interleaved reddish-brown, fine- to medium-grained, weakly to moderately foliated granite and amphibolite; restricted to the southern part of the map area.

Xgc Megacrystic-granitic gneiss (Paleoproterozoic) Pale-brown to reddish-brown, coarse-grained (megacrystic) weakly to moderately foliated gneiss; consists mainly of potassium feldspar, plagioclase, quartz, hornblende, and biotite; potassium feldspar grains are as much as 5 cm long; typically highly fractured and weathered reddish-brown near Cambrian nonconformity.

Xum Mafic and ultramafic rocks (Paleoproterozoic) Dark-gray, strongly foliated, fine- to medium-grained amphibolite consisting of plagioclase, hornblende, pyroxene, and biotite; generally found as small concordant bodies interleaved with Xgc and Xmgf. Also includes bodies of medium- to coarse-grained biotite, hydrobiotite, and vermiculite, intruded by migmatitic dikes from Xgn; this assemblage was probably metasomatized from an assemblage of hypersthene, diopside, hornblende, biotite, olivine, actinolite, and calcic plagioclase (Leighton, 1967).

Xog Orthogneiss (Paleoproterozoic) Strongly foliated gneiss containing plagioclase, quartz, hypersthene, potassium feldspar, biotite, and clinopyroxene; equivalent to the charnockite gneiss of Volborth (1962). Includes leucocratic portions in which foliation is weakly developed or absent, possibly equivalent to the migmatitic portions of Xgn (Fryxell et al., 1992).

Xgn Garnet gneiss (Paleoproterozoic) Strongly foliated gneiss and migmatite, contains garnet, biotite, cordierite, sillimanite, plagioclase, orthoclase, quartz, hercynite, and magnetite (Volborth, 1962; Thomas et al., 1988), migmatitic portions contain variably thick (1 cm to > 10 m) leucosome layers of very coarse grained quartz, feldspar, and garnet, with no internal fabric. Garnet porphyroblasts are generally unaltered, and surrounded by halos of quartz and feldspar, forming striking white-on-red contacts; westward from the west edge of the quadrangle, the garnet porphyroblasts become increasingly retrogressively altered to chlorite and mafic minerals (Fryxell et al., 1992). Similar gneiss crops out in the northern Virgin Mountains (Beal, 1965), at the west end of Frenchman Mountain, and to the south and west of this quadrangle (Blacet, 1975; Anderson et al., 1985; Thomas et al., 1988; Wooden and Miller, 1990; Wallace et al., 2005). K/Ar and Rb/Sr ages of 1.7 Ga were determined from pegmatites within unit Xgn (Wasserburg and Lanphere, 1965).

REFERENCES

Anderson, J.L., 1983, Proterozoic anorogenic granite plutonism of North America, *in* Medaris, L.G., Jr., Byers, C.W., Mickelson, D.M. and Shanks, W.C., editors, Proterozoic geology; selected papers from an international Proterozoic symposium: Boulder, Colorado, Geological Society of America Memoir 161, p. 133–154.

Anderson, R.E., Duebendorfer, E.M., and Sharp, W.D., 2001, Variation in displacement along strike of the South Virgin–White Hills detachment fault; perspective from the northern White Hills, northwestern Arizona; discussion and reply: Geological Society of America Bulletin, v. 113, p. 532–535.

Anderson, R.E., Longwell, C.R., Armstrong, R.L., and Marvin, R.F., 1972, Significance of K/Ar ages of Tertiary rocks from the Lake Mead region, Nevada–Arizona: Geological Society of America Bulletin, v. 83, p. 273–287.

Anderson, J.L., Young, E.D., Clarke, H.S., Orrell, S.E., Winn, M., Schmidt, C.S., Weber, M.E., and Smith, E.I., 1985, The geology of the McCullough Range wilderness area, Clark County, Nevada, Technical Report, University of Southern California, Los Angeles, 26 p.

Beal, L.H., 1965, Geology and mineral deposits of the Bunkerville mining district, Clark County, Nevada: Nevada Bureau of Mines and Geology Bulletin 63, 96 p.

Beard, L.S., 1996, Paleogeography of the Horse Spring Formation in relation to the Lake Mead fault system, Virgin Mountains, Nevada and Arizona, *in* Beratan, K., editor., Reconstructing the history of Basin and Range extension using sedimentology and stratigraphy: Boulder, Colorado, Geological Society of America Special Paper 303, p. 27–60.

Bennett, V.C., and DePaolo, D.J., 1987, Proterozoic crustal history of the Western United States as determined by neodymium isotopic mapping: Geological Society of America Bulletin, v. 99, p. 674–685.

Bernet, M., Brandon, M., Garver, J., Reiners, P., and Fitzgerald, P.G., 2002, Determining the zircon fission-track closure temperature: Geological Society of America Abstracts with Programs, v. 35, p. 18.

Billingsley, G.H., 1997, The Permian clastic sedimentary rocks of northwestern Arizona, *in* Maldonado, F., and Nealey, L.D., editors, Geologic studies in the Basin and Range–Colorado Plateau transition in southeastern Nevada, southwestern Utah, and northwestern Arizona, 1995: U.S. Geological Survey Bulletin B2153, p. 106–124.

Blacet, P.M., 1975, Preliminary geologic map of the Garnet Mountain quadrangle, Mohave County, Arizona: U.S. Geological Survey Open-File Report, 1:48,000.

Bohannon, R.G., 1983, Mesozoic and Cenozoic tectonic development of the Muddy, North Muddy, and northern Black Mountains, Clark County, Nevada, *in* Todd, V.R. and Howard, K.A., editors, Tectonic and stratigraphic studies in the eastern Great Basin: Boulder, Colorado, Geological Society of America Memoir 157, p. 125–148.

Bohannon, R.G., 1984, Nonmarine sedimentary rocks of Tertiary age in the Lake Mead region, southeastern Nevada and northwestern Arizona: U.S. Geological Survey Professional Paper 1259, 72 p.

Bohannon, R.G., 1992, Geologic map of the Red Pockets quadrangle, Mohave County, Arizona: U.S. Geological Survey Miscellaneous Investigations Series I-2288, 1:24,000.

Bowyer, B., 1958, Structural geology of the South Virgin Mountains, Clark County, Nevada: Geological Society of America Bulletin, v. 69, p.1538.

Brady, R.J., 1998, The geology of the Gold Butte breakaway zone and the mechanical evolution of normal fault systems [Ph.D. thesis]: California Institute of Technology, Pasadena, 200 p.

Brady, R., Wernicke, B., and Fryxell, J., 2000, Kinematic evolution of a large-offset continental normal fault system, South Virgin Mountains, Nevada: Geological Society of America Bulletin, v. 112, p. 1375–1397.

Burchfiel, B.C., Fleck, R.J., Secor, D.T., Vincelette, R.R., and Davis, G.A., 1974, Geology of the Spring Mountains, Nevada: Geological Society of America Bulletin, v. 85, p. 1013–1022.

Carpenter, D.G., Carpenter, J.A., Bradley, M.D., Franz, U.A., and Reber, S.J., 1989, On the role of isostasy in the evolution of normal fault systems; discussion: Geology, v. 17, p. 774–775.

Cole, E.D., 1989, Petrogenesis of late Cenozoic alkalic basalt near the eastern boundary of the Basin and Range; upper Grand Wash Trough, Arizona and Gold Butte, Nevada [M.S. thesis]: University of Nevada, Las Vegas, 68 p.

Damon, P.E., Shafiqullah, M., and Scarborough, R.B., 1978, Revised chronology for critical stages in the evolution of the lower Colorado River: Geological Society of America

Abstracts with Programs, v. 10, p. 101–102.

Darton, N.H., 1910, A reconnaissance of parts of northwestern New Mexico and northern Arizona: U.S. Geological Survey Bulletin 435, 88 p., 1:1,000,000.

Duebendorfer, E.M., and Sharp, W.D., 1998, Variation in displacement along strike of the South VirginWhite Hills detachment fault; perspective from the northern White Hills, northwestern Arizona: Geological Society of America Bulletin, v. 110, p. 1574–1589.

Dula, W.F., 1991, Geometric models of listric normal faults and rollover folds: American Association of Petroleum Geologists Bulletin, v. 75, p. 1609–1625.

Elliott, D.K., and Johnson, H.G., 1997, Use of vertebrates to solve biostratigraphic problems; examples from the lower and middle Devonian of western North America, *in* Klapper, G., Murphy, M.A., and Talent, J.A., editors, Paleozoic sequence stratigraphy, biostratigraphy, and biogeography; studies in honor of J. Granville ("Jess") Johnson: Geological Society of America Special Paper 321, p. 179–188.

Faulds, J.E., Price, L.M., and Wallace, M.A., 2001a, Pre-Colorado River paleogeography and extension along the Colorado Plateau–Basin and Range boundary, Northwestern Arizona, *in* Young, R.A, and Spamer, E.E., editors, Colorado River: Origin and evolution: Grand Canyon Association Monograph 12, p. 93–99.

Faulds, J.E., Wallace, M.A., Gonzalez, L.A., and Heizler, M.T., 2001b, Depositional environment and paleogeographic implications of the late Miocene Hualapai Limestone, northwestern Arizona and southern Nevada, *in* Young, R.A, and Spamer, E.E., editors, Colorado River: Origin and evolution: Grand Canyon Association Monograph 12, p. 81–87.

Fitzgerald, P.G., Fryxell, J.E., and Wernicke, B.P., 1991, Miocene crustal extension and uplift in southeastern Nevada; constraints from fission track analysis: Geology, v. 19, p. 1013–1016.

Fryxell, J.E., and Duebendorfer, E.M., 2005, Origin and trajectory of the Frenchman Mountain block, an extensional allochthon in the Basin and Range Province, southern Nevada: Journal of Geology, v. 113, p. 355–371.

Fryxell, J.E., Salton, G.G., Selverstone, J., and Wernicke, B., 1992, Gold Butte crustal section, South Virgin Mountains, Nevada: Tectonics, v. 11, p. 1099–1120.

Gilbert, G.K., 1875, U.S. Geological and Geographical Survey W. 100th Meridian, v. 3, p. 162–197.

Hamblin, W.K., 1965, Origin of "reverse drag" on the downthrown side of normal faults: Geological Society of America Bulletin, v. 76, p. 1145–1164.

Hewett, D.F., 1931, Geology and ore deposits of the Goodsprings quadrangle, Nevada: U.S. Geological Survey Professional Paper 162, 172 p., 1:62,500.

Howard, K.A., Faulds, J.E., Beard, L.S., and Kunk, M.J., 2000, Reverse-drag folding across the path of the antecedent early Pliocene Colorado River below the mouth of the Grand Canyon; implications for plateau uplift: Geological Society of America Abstracts with Programs, v. 32, p. 41.

Howard, K.A., Hook, S.J., Phelps, G.A., and Block, D.L., 2003, Geologic map of the Hiller Mountains quadrangle, Clark County, Arizona: Nevada Bureau of Mines and Geology Map 137, 1:24,000.

Karlstrom, K.E., and Bowring, S.A., 1988, Early Proterozoic assembly of tectonostratigraphic terranes in southwestern North America: Journal of Geology, v. 96, p. 561–576.

Langenheim, R.L., Jr., 1963, Mississippian stratigraphy in southwestern Utah and adjacent parts of Nevada and Arizona, *in* Geology of southwestern Utah, Intermountain Association of Petroleum Geologists, 12th Annual Field Conference Guidebook, p. 30–41.

Lee, W.T., 1908, Geologic reconnaissance of a part of western Arizona: U.S. Geological Survey Bulletin 352, 96 p.

Leighton, F.B., 1967, Gold Butte vermiculite deposits, Clark County, Nevada: Nevada Bureau of Mines and Geology Report 16, 18 p., 1:4,800.

Longwell, C.R., 1921, Geology of the Muddy Mountains, Nevada, *with a section on* the Grand Wash Cliffs in western Arizona: American Journal of Science, v. 1, p. 39–62.

Longwell, C.R., 1936, Geology of the Boulder Reservoir floor: Geological Society of America Bulletin, v. 47, p. 1393–1476.

Longwell, C.R., 1945, Low-angle normal faults in the Basin and Range province: Eos (Transactions, American Geophysical Union), v. 26, p. 107–118.

Longwell, C.R., 1949, Structure of the northern Muddy Mountain area, Nevada: Geological Society of America Bulletin, v. 60, p. 923–967.

Longwell, C.R., Pampeyan, E.H., Bowyer, B., and Roberts, R.J., 1965, Geology and mineral deposits of Clark County, Nevada: Nevada Bureau of Mines Bulletin 62, 218 p.

Lucchitta, I., 1966, Cenozoic geology of the upper Lake Mead area adjacent to the Grand Wash Cliffs, Arizona [Ph.D. thesis]: Pennsylvania State University, University Park, 274 p.

Lucchitta, I., and Young, R.A., 1986, Structure and geomorphic character of western Colorado Plateau in the Grand Canyon–Lake Mead region, *in* Nations, J.D., Conway, C.M., and Swann G.A., editors, Geology of central and northern Arizona: Geological Society of America, Rocky Mountain Section Guidebook, Flagstaff, Northern Arizona University, p. 159–176.

Lumsden, D.N., Ledbetter, M.T., and Smith, G.T., 1973, Lithostratigraphic analysis of the Bird Spring-Callville Group and Pakoon Formation (Pennsylvanian-lower Permian), southern Clark County, Nevada: Journal of Sedimentary Petrology, v. 43, p. 655–671.

Matthews, J., 1976, Paleozoic stratigraphy and structural geology of the Wheeler Ridge area, northwestern Mohave County, Arizona [M.S. thesis]: Northern Arizona University, Flagstaff, 145 p.

McKee, E.D., 1934, The Coconino sandstone; its history and origin: Carnegie Institution of Washington Publication 440, p. 78–115.

McKee, E.D., 1938, The environment and history of the Toroweap and Kaibab formations of northern Arizona and southern Utah: Carnegie Institution of Washington Publication 492, 268 p.

McKee, E.D., 1945, Stratigraphy and ecology of the Grand Canyon Cambrian, Part 1 of Cambrian history of the Grand Canyon region: Carnegie Institution of Washington Publication 563, p. 3–168.

McKee, E.D., 1963, Nomenclature for lithologic subdivisions of the Redwall Limestone, Arizona: U.S. Geological Survey Professional Paper 475-C, p. 21–22.

McKee, E.D., 1969, Stratified rocks of the Grand Canyon, *in* U.S. Geological Survey, The Colorado River region and John Wesley Powell: U.S. Geological Survey Professional Paper 669-B, p. 222–249.

McKee, E.D., 1975, The Supai Group; subdivision and nomenclature: U.S. Geological Survey Bulletin 1395-J, 11 p.

McNair, A.H., 1951, Paleozoic stratigraphy of part of northwestern Arizona: American Association of Petroleum Geologists Bulletin, v. 35, p. 503–541.

Morgan, J.R., 1968, Structure and stratigraphy of the northern part of the South Virgin Mountains, Clark County, Nevada [M.S. thesis]: University of New Mexico, Albuquerque, 103 p.

Noble, L.F., 1914, The Shinumo quadrangle, Grand Canyon district, Arizona: U.S. Geological Survey Bulletin 549, 100 p., 1:48,000.

Parolini, J.R., Smith, E.I., and Wilbanks, J.R., 1981, Fission track dating of rapakivi granite in the Rainbow Gardens and in the South Virgin Mountains, Clark County, Nevada: Isochron/West, v. 30, p. 9–10.

Reiners, P.W., 2002, (U-Th)/ He chronometry experiences a renaissance: Eos (Transactions, American Geophysical Union), v. 83, p. 26–27.

Reiners, P.W., Brady, R.J., Farley, K.A., Fryxell, J.E., Wernicke, B., and Lux, D., 2000, Helium and argon thermochronometry of the Gold Butte Block, South Virgin Mountains, Nevada: Earth and Planetary Science Letters, v. 178, p. 315–326.

Reiners, P.W., Farley, K.A., and Hickes, H.J., 2002, He diffusion and (U-Th)/He thermochronometry of zircon; initial results from Fish Canyon Tuff and Gold Butte: Tectonophysics, v. 349, p. 297–308.

Rowland, S.M., Parolini, J.R., Eschner, E., McAllister, A.J., and Rice, J.A., 1990, Sedimentologic and stratigraphic constraints on the Neogene translation and rotation of the Frenchman Mountain structural block, Clark County, Nevada, *in* Wernicke, B.P., editor, Basin and Range extensional tectonics near the latitude of Las Vegas, Nevada: Boulder, Colorado, Geological Society of America Memoir 176, p. 99–122.

Schenk, E.T., and Wheeler, H.E., 1942, Cambrian sequence in western Grand Canyon, Arizona: Journal of Geology, v. 50, p. 882–899.

Shafiqullah, M., Damon, P.E., Lynch, D.J., Reynolds, S.J., Rehrig, W.A., and Raymond, R.H., 1980, K/ Ar geochronology and geologic history of southwestern Arizona and adjacent areas: Studies in western Arizona, v. 12, p. 201–260.

Silver, L.T., Bickford, M.E., Van Schmus, W.R., Anderson, J.L., Anderson, T.H., and Medaris, L.G, Jr., 1977, The 1.4–1.5 b.y. transcontinental anorogenic plutonic perforation of North America: Geological Society of America Abstracts with Programs, v. 9, p.1176–1177.

Stewart, J.H., 1980, Geology of Nevada; a discussion to accompany the geologic map of Nevada: Nevada Bureau of Mines and Geology Special Publication 4, 132 p.

Thomas, W.M., Clark, S.H., Young, E.D., Orrell, S.E., and Anderson, J.L., 1988, Proterozoic high-grade metamorphism in the Colorado River region, Nevada, Arizona, and California, *in* Ernst, W.G., ed., Metamorphism and crustal evolution of the western United States, Rubey Volume VII: Prentice Hall, Englewood Cliffs, N.J., p. 526–537.

Volborth, A., 1962, Rapakivi-type granites in the Precambrian complex of Gold Butte, Clark County, Nevada: Geological Society of America Bulletin, v. 73, p. 813–831.

Wallace, M., Faulds, J.E., and Brady, R., 2005, Geologic map of the Meadview North quadrangle, Mohave County, Arizona and Clark County, Nevada: Nevada Bureau of Mines and Geology Map 154, 1:24,000.

Wasserburg, G.J., and Lanphere, M.A., 1965, Age determinations in the Precambrian of Arizona and Nevada: Geological Society of America Bulletin, v. 76, p. 735–758.

Wheeler, H.E., 1943, Lower and middle Cambrian stratigraphy in the Great Basin area: Geological Society of America Bulletin, v. 54, p. 1781–1822.

Wheeler, H.E., and Beesley, E.M., 1948, Critique of the time-stratigraphic concept [Bright Angel group, southwestern U.S.]: Geological Society of America Bulletin, v. 59, p. 75–85.

White, D., 1929, Flora of the Hermit Shale, Grand Canyon, Arizona: Carnegie Institution of Washington Publication 405, 219 p.

Wooden, J.L., and Miller, D.M., 1990, Chronologic and isotopic framework for early Proterozoic crustal evolution in the eastern Mojave Desert region, SE California: Journal of Geophysical Research, v. 95, p. 20133–20146.

Suggested citation:

Brady, R.J., Fryxell, J.E., Wernicke, B.P., 2011, Geologic map of the Iceberg Canyon quadrangle, Clark County, Nevada and Mohave County, Arizona, *with text entitled* Overview of the stratigraphy and structure of the Iceberg Canyon quadrangle, Clark County, Nevada and Mohave County, Arizona: Nevada Bureau of Mines and Geology Map 166, 1:24,000 scale, 16 p. text.